

Mathematical prediction of suspension bridge behavior in wind from dynamic section model tests

Autor(en): **Vincent, George S.**

Objektyp: **Article**

Zeitschrift: **IABSE publications = Mémoires AIPC = IVBH Abhandlungen**

Band (Jahr): **12 (1952)**

PDF erstellt am: **03.05.2024**

Persistenter Link: <https://doi.org/10.5169/seals-12327>

Nutzungsbedingungen

Die ETH-Bibliothek ist Anbieterin der digitalisierten Zeitschriften. Sie besitzt keine Urheberrechte an den Inhalten der Zeitschriften. Die Rechte liegen in der Regel bei den Herausgebern.

Die auf der Plattform e-periodica veröffentlichten Dokumente stehen für nicht-kommerzielle Zwecke in Lehre und Forschung sowie für die private Nutzung frei zur Verfügung. Einzelne Dateien oder Ausdrucke aus diesem Angebot können zusammen mit diesen Nutzungsbedingungen und den korrekten Herkunftsbezeichnungen weitergegeben werden.

Das Veröffentlichen von Bildern in Print- und Online-Publikationen ist nur mit vorheriger Genehmigung der Rechteinhaber erlaubt. Die systematische Speicherung von Teilen des elektronischen Angebots auf anderen Servern bedarf ebenfalls des schriftlichen Einverständnisses der Rechteinhaber.

Haftungsausschluss

Alle Angaben erfolgen ohne Gewähr für Vollständigkeit oder Richtigkeit. Es wird keine Haftung übernommen für Schäden durch die Verwendung von Informationen aus diesem Online-Angebot oder durch das Fehlen von Informationen. Dies gilt auch für Inhalte Dritter, die über dieses Angebot zugänglich sind.

Mathematical Prediction of Suspension Bridge Behavior in Wind from Dynamic Section Model Tests

*Vorausberechnung des Verhaltens von Hängebrücken im Wind, auf Grund von
dynamischen Querschnittsmodellversuchen*

*La prévision mathématique du comportement des ponts suspendus, sous l'action
du vent, à partir d'essais dynamiques sur modèles de sections*

GEORGE S. VINCENT, Principal Highway Bridge Engineer, United States Bureau of
Public Roads, Washington

When the engineers of the Washington Toll Bridge Authority undertook the task of rebuilding the Tacoma Narrows Bridge, their first concern was to determine the nature of the wind action which had oscillated it harmlessly for a few months and finally destroyed it on November 7, 1940, and, by using this knowledge, insure the new bridge against such action. A mechanical model had been built which demonstrated the natural modes of oscillation of the bridge and formulas were developed for predicting them (see fig. 1). Some study of the effects of mechanical damping had been made with this model. Static wind tunnel tests had been made on section models of the bridge to determine the lift, drag, and moment coefficients. These investigations led to tentative though inadequate theories regarding the mechanics of the excitation. It was eventually determined that a properly scaled complete model of the bridge should be tested in a wind tunnel¹⁾ ²⁾ ³⁾).

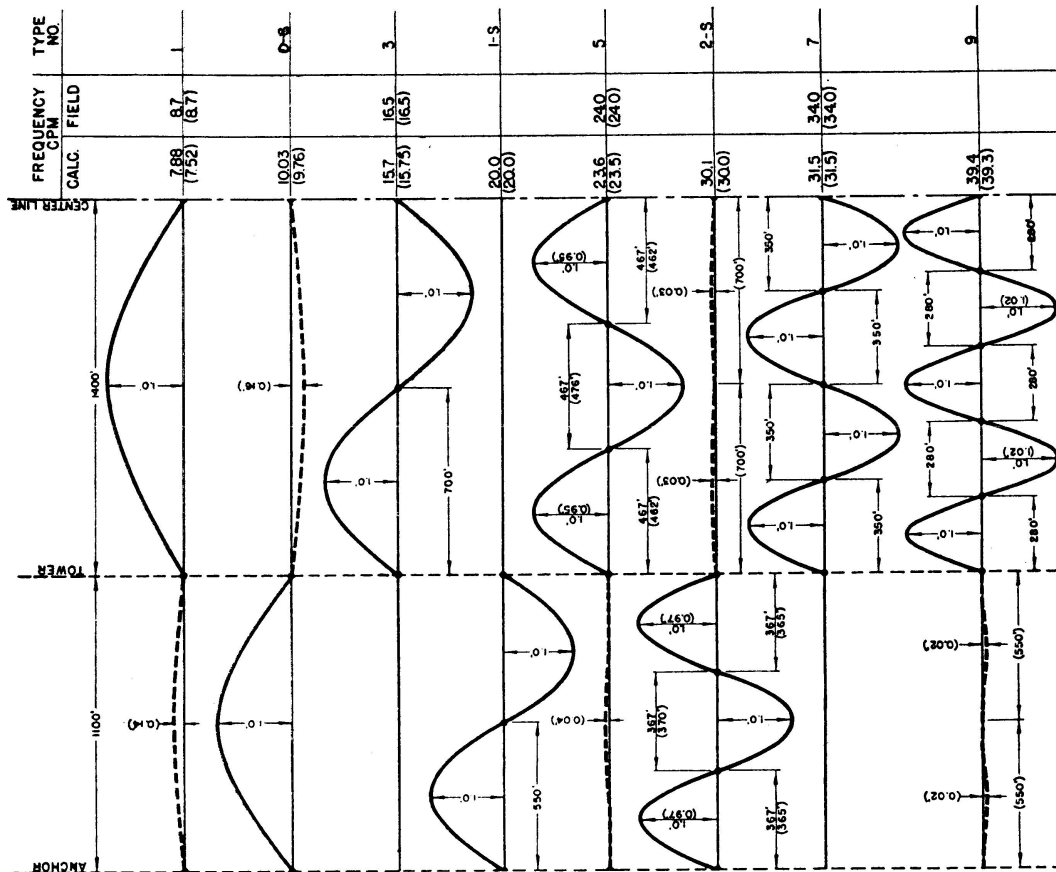
The model was constructed to a linear scale of 1 to 50, making it 100 ft. long (2800 ft. main span and two 1100 ft. side spans) and tested in a specially built wind tunnel having a throat 100 ft. long and 4 ft. high. A review of the scales of the various properties and elements involved will give some conception of the model and tests. The linear scale, n (1/50 in this case), and its powers, of course govern the spatial dimensions. The acceleration of gravity, g , acts alike on the model and prototype and so has the scale of unity. To make

¹⁾ "Aerodynamic Stability of Suspension Bridges with Special Reference to the Tacoma Narrows Bridge", University of Washington Bulletin No. 116, "Part I — Investigations Prior to October, 1941" by F. B. FARQUHARSON.

²⁾ Ibid. "Part II — Mathematical Analyses" by F. C. SMITH and GEORGE S. VINCENT.

³⁾ Ibid. "Part III — The Investigation of Models of the Original Tacoma Narrows Bridge under the Action of Wind" by F. B. FARQUHARSON.

ASYMMETRIC MODES



SYMMETRIC MODES

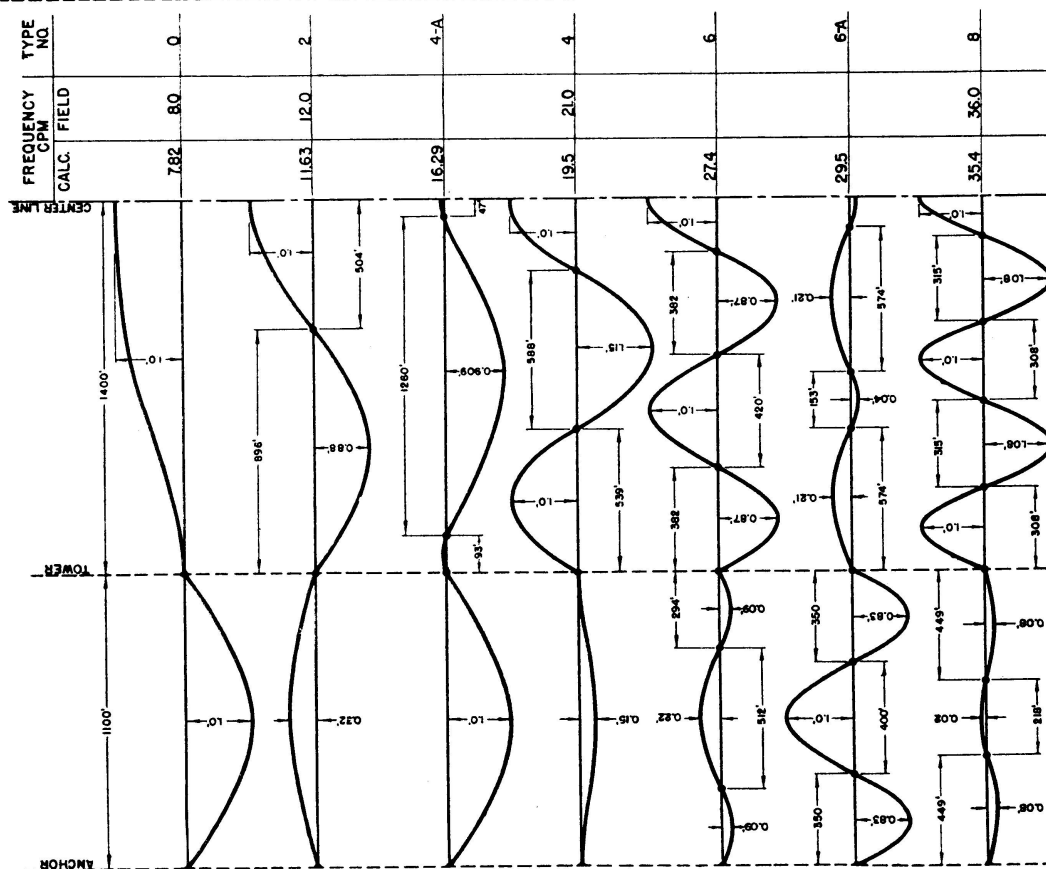


Fig. 1. Wave Forms for Original Tacoma Narrows Bridge. (Broken lines and figures in parentheses represent modified condition with mid-point of main cable tied to suspended structure so as to prevent relative longitudinal motion between them)

inertial forces proportional to gravitational forces the scale of all accelerations, a , must likewise be unity which leads to the scale of \sqrt{n} for time, t , and for velocity, V . Natural air being used in the wind tunnel, it is desirable that the scale of mass density, ρ , be unity which determines the scale, n^3 , for the mass, m , of each element of the structure. This leads to correct mass distribution and makes n^3 the scale of weight, w , and of a force, F .

These scales involve no problems except in the properties of the materials. Modulus of elasticity, force divided by area, requires the scale, n . Material having a modulus of elasticity $1/50$ that of steel while having at the same time the required density, strength and damping properties is not available. However, the modulus of elasticity is involved only in combination with area, A , where direct stress is involved and with moment of inertia, I , where bending is involved, and the solution was to use steel, making the scale of modulus of elasticity unity and to distort the scales of A and I for stress-carrying elements to n^3 and n^5 , respectively. Accordingly, the cable consisted of piano wire whose area was $(1/50)^3$ times that of the prototype cable, enclosed in a jointed steel sleeve whose diameter was $1/50$ that of the prototype cable. Also girders and trusses were made up in separate sections each attached only at one point to a much smaller continuous bar having a moment of inertia $(1/50)^5$ times that of the prototype flexural member. The decks were jointed to prevent their contributing to both vertical and lateral stiffness. All details and connections of the model including the separate sections described above were designed to minimize structural damping and so secure a sensitive response to wind action³).

The scales described above are based on the assumption that the flow around the model is turbulent and that the wind forces vary in accordance with Froude's Law, the influence of Reynolds' Number being unimportant. The validity of this assumption was reasonably demonstrated by the agreement between the model behavior and that of the original Tacoma Narrows Bridge as imperfectly revealed by observations made during its brief life. There is some uncertainty concerning the wind measurements made at only one point on the bridge and often the motion of the bridge altered before sufficient measurements could be made to establish its character but the composite indication of all of the field observations served to establish confidence in the full model tests as a means of determining what the prototype would do in a known wind stream. Later, static tests made on section models over a wide range of Reynolds' Number showed no appreciable scale effect⁴). Also, the form of the curve of the logarithmic decrement for aerodynamic damping in still air (discussion of fig. 8) reveals only a minor influence of viscous forces in the wind.

⁴) These studies will be described in Part IV of University of Washington, Bulletin No. 116, now in preparation.

The validity of the full model tests having been established by the investigation of the original bridge, a full model of the proposed new bridge was built and similarly tested. It became apparent that some improvement in the aerodynamic stability of this design was necessary and the effects of various alterations were tested, leading ultimately to the design finally adopted. The numerous configurations were first tried out on a section model, equivalent to a five-foot section of the suspended structure of the full model, mounted on springs designed to produce torsional or vertical oscillation at the frequency of some convenient mode of the full model (see fig. 1). The configuration selected on the basis of these tests was then installed on the full model and its beneficial effect was verified by full model tests⁵).

From the start, the tests demonstrated the proportionality of the wind velocity, V , and the frequency, N , of the oscillation caused by the wind. To make it dimensionless and independent of the scale their ratio is divided by the width, b , resulting in the ratio, V/Nb , critical values of which are essentially constant for a given section and a given type of motion. For example, all vertical modes will begin at wind velocities corresponding to the critical V/Nb ratio for vertical modes and there is a different critical V/Nb ratio for torsional modes. Similarly all modes of the same type reach their maximum amplitudes at about the same V/Nb ratio and their upper critical velocities at which motion dies out fall close to a common V/Nb ratio. Differences in aspect ratio (length of model to its width) and in tunnel wall conditions cause minor shifts in the critical ratio. Changes in shape affect it profoundly. Increasing the structural damping increases the critical V/Nb ratio at which a catastrophic oscillation starts but has small effect on that of a restricted oscillation (though it limits the maximum amplitude reached by the latter).

The indications of the full and section model tests were quite similar although they differed quantitatively because of certain essential differences in the models, principally the following:

1. The structural damping was greater on the full model than on the section model (except in certain tests for which the damping of the section model mounting was progressively increased).
2. The movement was uniform along the section model but the amplitude on the full model, of course, varied in accordance with the wave form of the particular mode. Figure 1 shows typical forms for several modes.

The effects of the above factors can be evaluated mathematically. In addition there is a small effect from the wind flow around the ends of the section model. Tests with and without end plates blocking this end flow showed that its effect was very small if the aspect ratio was as much as 4.5. There was some minor uncertainty concerning the uniformity of the wind along the full model, particularly, the angle of attack, β , the divergence of the wind stream

⁵) Ibid.

from the horizontal. This angle was controlled by the adjustment of horizontal vanes arranged in 25 sets each 4 ft. long. The pitchmeters and smoke streamers used for measuring the angle of attack permitted variations of as much as 1° in the actual setting of the angle. Also the curvature of the wind downstream from the model caused a small change in β as the velocity increased. The effects of these factors differed in the various tests depending upon the sensitivity of the phenomenon to the angle of attack.

Test Procedure and Analysis of Data

For predicting bridge behavior in the wind the section model is used as an instrument for determining the rate of energy transfer between the structure and the wind stream. The logarithmic decrement, δ , easily determined from the record of motion of the model, is the key to the analysis because of its relation to ψ , the rate of energy change per cycle. For low damping $\delta = \psi/2$. If δ exceeds about 0.05, a closer approximation is:

$$\psi = 2\delta(1 - \delta/2) \quad (1)$$

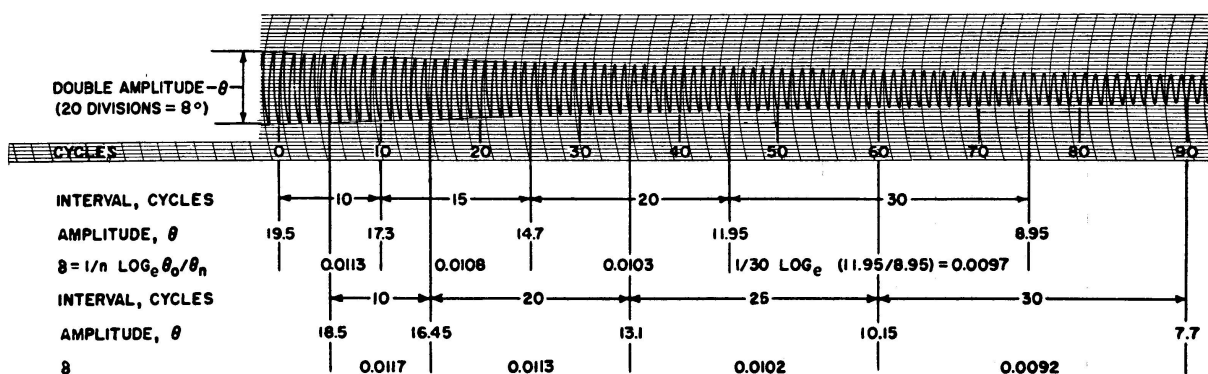


Fig. 2. Specimen Oscillograph Record and Calculations of Logarithmic Decrement

The logarithmic decrement is defined as the natural logarithm of the ratio of two successive amplitudes and is computed from the formula:

$$\delta = \frac{1}{n} \log_e \frac{\eta_0}{\eta_n} \quad (2)$$

in which η_0 is a conveniently chosen amplitude and η_n is the amplitude n cycles later. Figure 2 shows the detailed procedure for determining δ using a double series of measurements to provide a check and detect discrepancies. For viscous damping δ is constant with respect to amplitude. For Coulomb friction damping it varies inversely with amplitude and for damping due to a force proportional to the square of the velocity of vibration δ is directly proportional to amplitude. It is positive for decreasing and negative for increasing amplitude.

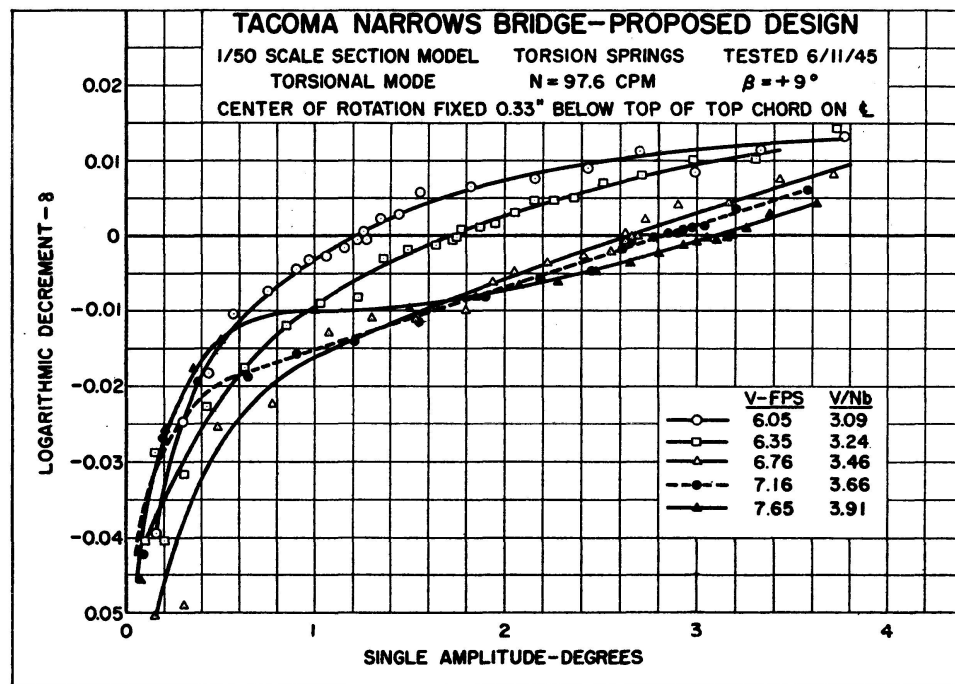


Fig. 3. Typical Logarithmic Decrement Curves from Section Model Tests

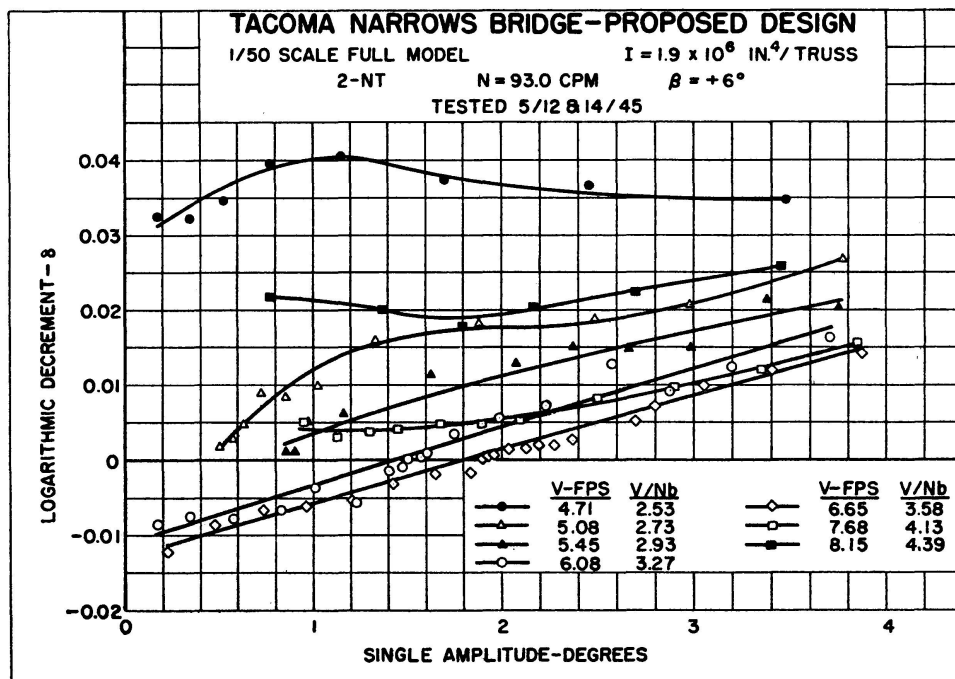


Fig. 4. Typical Logarithmic Decrement Curves from Full Model Tests

The value determined by section model tests may also be defined:

$$\delta = \delta_s + \delta_a \quad (3)$$

in which δ_s is the structural damping (in springs and mounting) and δ_a is the aerodynamic or atmospheric damping. The former is always positive. The

latter is positive in still air and may be positive or negative in a wind depending upon the velocity and vertical angle of attack, β . Figures 3 and 4 show curves for δ plotted against the amplitude in degrees of a torsional oscillation. These are typical curves for restricted oscillations as plotted from early tests. It will be noted that they do not correspond because the angle of attack differs.

When δ is zero no change in amplitude is taking place. Therefore, the intersections of the curves with the axis of zero δ indicate the "steady state" amplitudes for the corresponding velocities. The model at rest in the wind stream will build up to this amplitude and if manually excited to a greater amplitude it will decay to this steady state.

These individual curves showing the influence of velocity and amplitude upon the rate of energy transfer suggested the method of prediction described herein. It was recognized, however, that only the aerodynamic damping was caused by forces which could be correctly scaled in the model tests. The structural make-up and action of the model differ so much from those of the prototype that their structural dampings bear no useful quantitative relationship. The section model tests do show how structural damping will affect the oscillation, but they give no quantitative indication of what the structural damping of the prototype will be. This must be determined by other means⁶⁾ ⁷⁾ or assumed for the purpose of analysis.

The first task was to segregate the aerodynamic and structural damping of the section model oscillating in still air. The method used was based on the knowledge that the section model was rigid due to its relatively short length, and deliberate stiffening in some cases, so that its structural damping was due entirely to the action of the springs and their supports and connections. The structural damping was therefore determined by recording the decay of oscillation when two streamlined brass rods were suspended from two of the springs constituting the support of one end of the model (see fig. 5). The rods were of such size that the total weight on the two springs was one-half that of the section model. The air forces (still air) were negligible. Having thus determined δ_s , δ_a was found by subtracting δ_s from δ as determined from the tests of the section model with the same suspension and frequency.

Though simple in principle the segregation of the aerodynamic damping involved numerous experimental difficulties and delays.

The model mounting including the spring suspension and restraining wires used in these tests is shown in figure 4 of the paper "Model Verification of the Classical Flutter Theory as Adapted to the Suspension Bridge" by Professor F. B. FARQUHARSON (page 147 of this volume). The oscillations of the brass

⁶⁾ "Damping Effect in Suspension Bridges" by ARNE SELBERG, Vol. X, Publications of the International Association for Bridge and Structural Engineering.

⁷⁾ Damping tests on small suspension bridges, intended to develop methods for use on major bridges will be described in Part V of University of Washington, Bulletin No. 116, in preparation.

weights were recorded on an oscillograph receiving the amplified output of an electrical circuit involving an unbonded wire strain gage which sustained a part of the reaction of the spring support. The oscillation of the section model was similarly recorded using the output of a linear differential transformer built into a small accelerometer placed on the model. In both cases the record was calibrated by adjusting the gain of the amplifier while manually maintaining a steady amplitude and observing a pointer attached to the oscillating

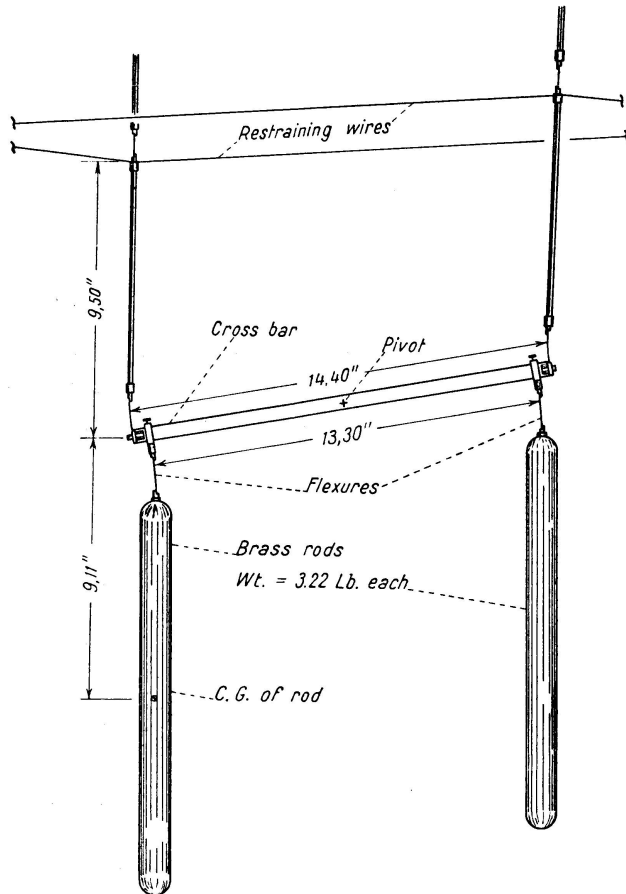


Fig. 5. Brass Rods Suspended on Spring Mounting for One End of Section Model

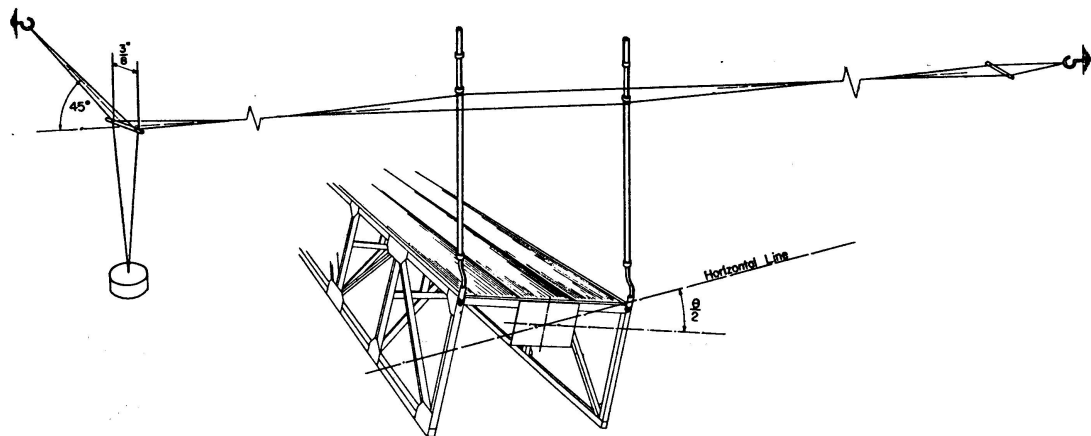


Fig. 6. Type II Restraining Wires

system as it moved across a fixed scale indicating the linear or angular motion. The restraining wires were used to prevent displacement and sway of the model in the direction of the wind. The type I wires resist torsional but not vertical motion, and use was made of this action in the studies of flutter. In the tests here reported, type II wires were used. These (shown in figures 5 and 6) restrained each hanger separately and being attached to supports some 8 or 10 ft. from the model they had negligible effect on vertical or torsional oscil-

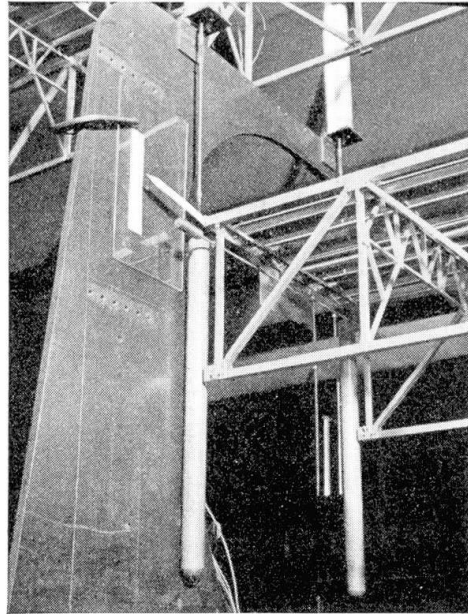


Fig. 7. Wood Rods Suspended from Section Model

lation. Torsional oscillation took place about a longitudinal axis of the model which usually tended to shift slightly in a small orbit with respect to the model. This caused a slight irregularity in the amplitude as recorded at one edge of the model. Fixing the axis of rotation within the observed orbit by means of a phonograph needle lightly pressed into a small hole or dimple in a plate attached to each end of the model gave a steadier record and had only a slight effect on the structural damping and the behavior of the model. The pivot plate is shown in figures 6 and 7. In the tests here described, the pivot was placed on the longitudinal centerline of the deck.

The assumption that the aerodynamic forces on the brass rods in still air were negligible was readily confirmed by suspending from the section model very light wood rods of the same size (fig. 7) and noting that the logarithmic decrement, δ , remained essentially the same as for the model alone.

Figure 8 shows both δ and δ_s plotted against amplitude for vertical oscillation in still air. The atmospheric damping, δ_a , is indicated by the ordinates between these curves. It will be noted that δ_a has a very small initial value and increases directly with the amplitude. This is significant as shown by the following analysis.

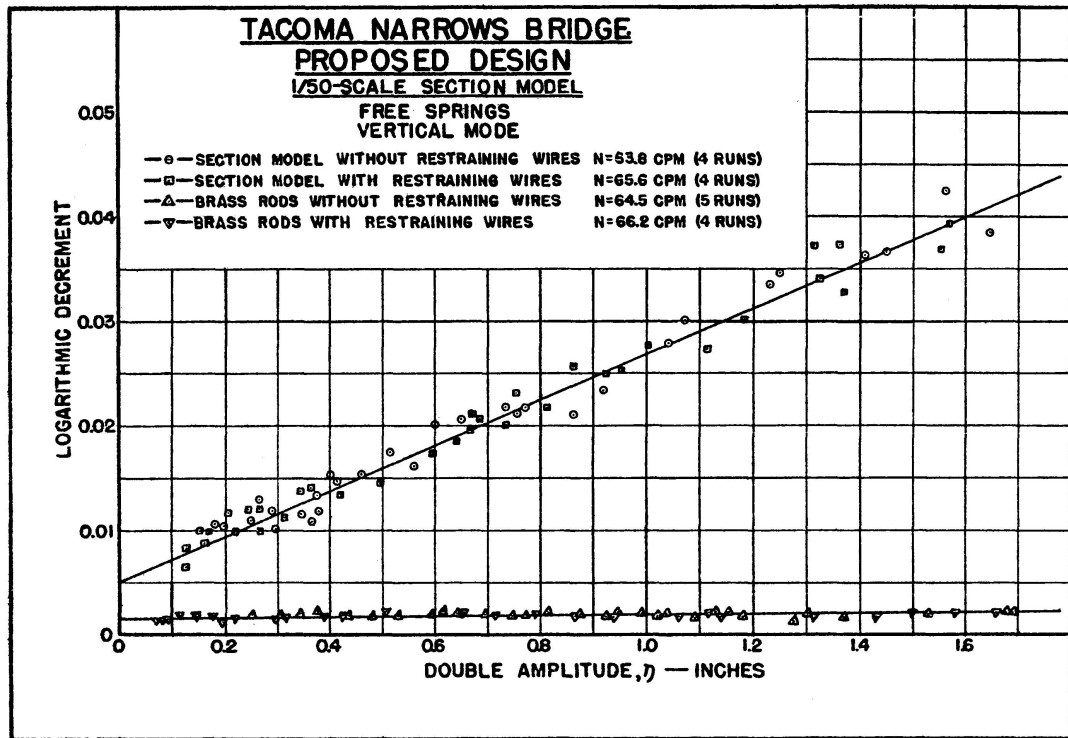


Fig. 8. Aerodynamic and Structural Logarithmic Decrements in Still Air as Functions of Amplitude. Vertical Oscillation

The energy of a vibrating system can be expressed:

$$U = \frac{m \omega^2 \eta^2}{2} \quad (4)$$

in which m is the mass, ω is the circular frequency and η is the amplitude. The work performed on the system by a force which varies as the square of the velocity of vibration is:

$$\Delta U = C m \omega^2 \eta^3 \quad (5)$$

in which C is an experimental constant. The resulting rate of change in energy per cycle then is:

$$\psi = \frac{\Delta U}{U} = \frac{C}{2} \eta \quad (6)$$

Thus ψ and δ_a should increase as linear functions of η . The experimental value shown in figure 8 may therefore be regarded as a small constant value due to viscous damping plus a much larger constituent due to the dynamic pressure. The small influence of the viscous damping confirms the validity of testing the models under Froude's Law. Curves for torsional oscillation in still air, shown in figure 9, show this same basic character but are curved somewhat because of the more complex air flow. The fact that this evidence of the dominance of inertial force action is not found in the curves obtained with the model in a wind stream need not be disturbing. Only in the still air tests is

the effective velocity identical to the velocity of vibration. In a wind stream the effective velocity is a resultant of velocities due to wind and to oscillation. Furthermore the air forces are altered by vortex action associated with the particular velocity and their energy contribution to the motion, depending upon the degree of resonance with the motion of the structure, changes with wind velocity and with amplitude. The resulting relation between amplitude and logarithmic decrement, therefore, is not simple.

Figure 9 shows the small effect on damping caused by the pivots fixing the center of rotation.

Theory Underlying Predictions

In developing the relation between the logarithmic decrement, δ_a , of the section model and that of the prototype it should be noted that the mass of the section model is uniformly distributed along its length and the motion is likewise the same at all cross sections of the model. Therefore, both U and ΔU (equations 4 and 5) are proportional to the length of model considered and their ratio $\Delta U/U = \psi$, is the same for any portion of the model, such as a unit length, as it is for the entire model. The value of ψ for a unit length of the full model at a location which moves with the same amplitude as the section model will be the same as ψ for the latter. Moreover, since the scales are correct, ψ , which is a non-dimensional ratio, will be the same for a unit length of the prototype when oscillating at an amplitude equal to that of the section model adjusted by the scale factor.

What has been said about ψ applies also to δ_a because of their relationship. This means that a curve for δ_a determined from section model tests and plotted as a function of the amplitude, η (as in fig. 8), will apply to the prototype if the abscissa scale is changed to the corresponding prototype amplitudes. For figure 8 η would be multiplied by fifty. For torsional oscillation as illustrated by figure 9 no change in the graph is required.

To avoid confusion, δ_a as a function of the amplitude of motion of a unit length of model or prototype will be designated, δ_{ma} , and can be expressed as the power series:

$$\delta_{ma} = A_{ma} + B_{ma} \eta + C_{ma} \eta^2 + D_{ma} \eta^3 \dots \quad (7)$$

in which A_{ma} , etc. are the coefficients required to define the curves plotted from the section model test data.

For the purpose of this analysis the approximation, $\psi = 2\delta$ is adequate and the energy change due to atmospheric damping on a differential length of the prototype is:

$$\Delta U = 2 \delta_{ma} \frac{m_p \omega^2 \eta^2}{2} dx \quad (8)$$

m_p being the mass of the prototype per unit length, ω its frequency and η its amplitude.

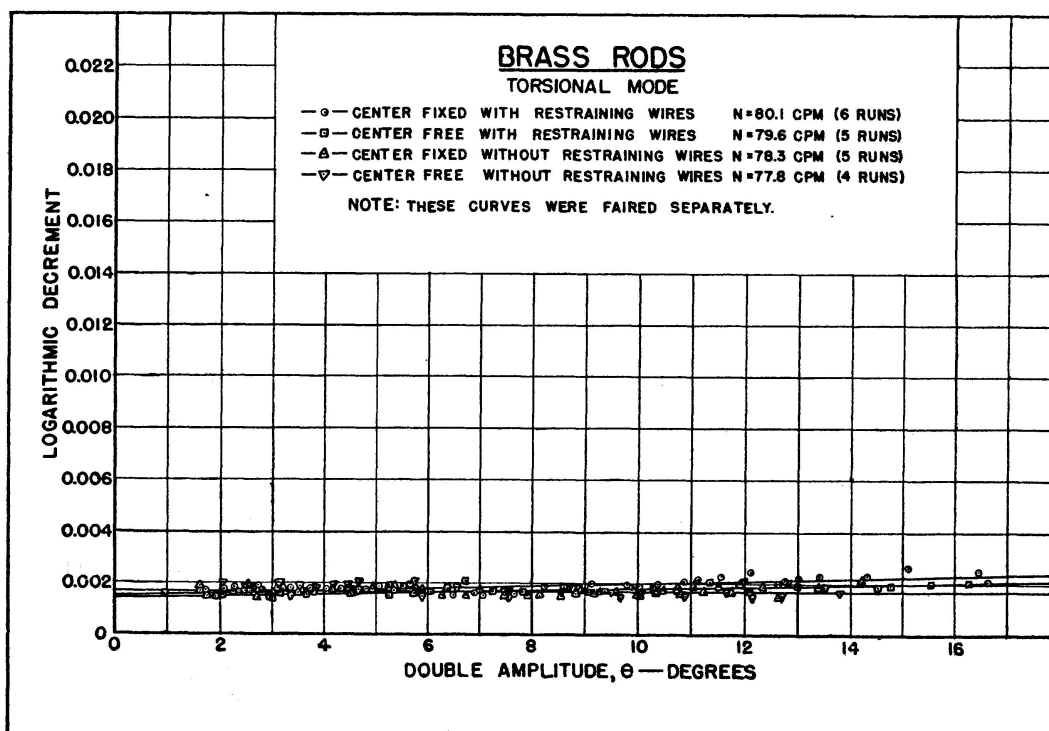
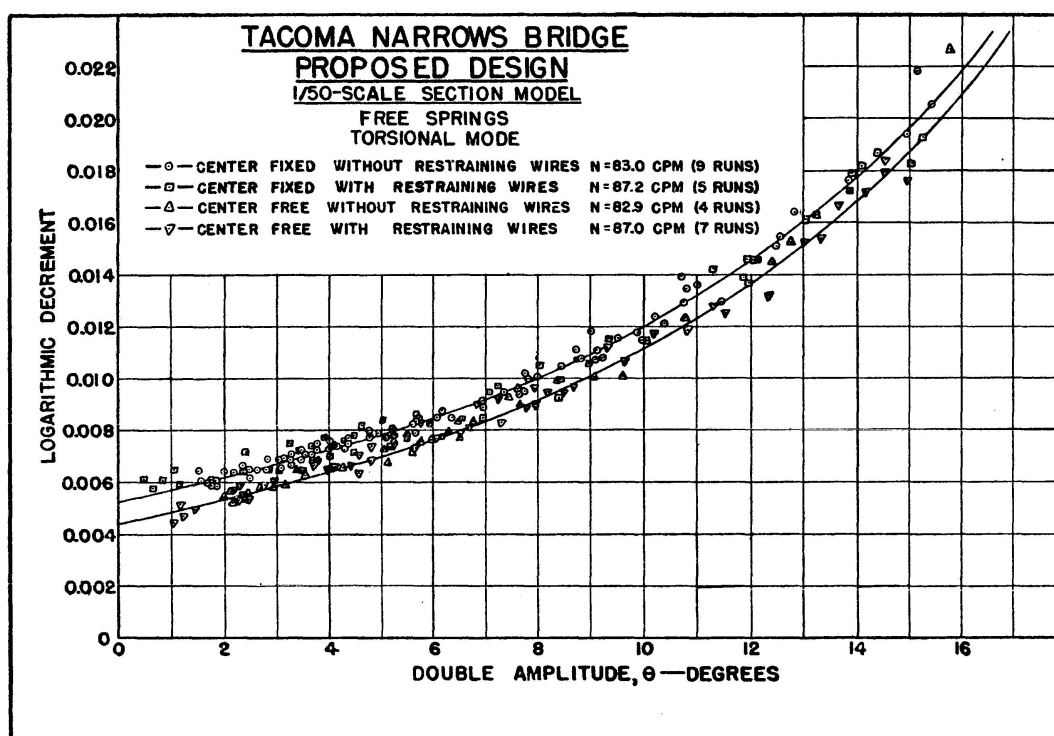


Fig. 9. Aerodynamic and Structural Logarithmic Decrements in Still Air as Functions of Amplitude. Torsional Oscillation

Mode and wave form		Coefficients for constants				
		B_{ma}	C_{ma}	D_{ma}	E_{ma}	F_{ma}
		$\int_L \eta^3 dx$	$\int_L \eta^4 dx$	$\int_L \eta^5 dx$	$\int_L \eta^6 dx$	$\int_L \eta^7 dx$
a	<p>1-NV Tower $l = 1100'$ $\eta_0 = 1.0$ $\eta = \eta_0 \sin \frac{\pi x}{l}$</p>	0,8488	0,7500	0,6791	—	—
b	<p>0-NV Tower $l = 1100'$ $\eta_0 = 1.0$ $\eta = \eta_0 \sin \frac{\pi x}{l}$</p> <p>M.S. — $\eta = 0,49729 \eta_0 (1 + 1,0109 \cos \frac{5,99x}{l})$ S.S. — $\eta = 0,49729 \eta_0 (1 + 1,3403 \cos \frac{5,99x}{l} + 2,2320 \sin \frac{5,99x}{l})$</p>	0,7702	0,6275	0,5306	0,4610	0,4090
c	<p>2-NV Tower $l = 1100'$ $\eta_0 = 1.0$ $\eta = \eta_0 \sin \frac{\pi x}{l}$</p>	0,7412	0,5965	0,5036	0,4377	0,3877

Table I. Integration Ratios

The total change in energy is:

$$\int_L \Delta U = \delta_{ma} m_p \omega^2 \int_L \eta^2 dx \quad (9)$$

in which L indicates integration over the entire length of the bridge. Substituting for δ_{ma} from equation (7) this becomes:

$$\int_L \Delta U = m_p \omega^2 \left[A_{ma} \int_L \eta^2 dx + B_{ma} \int_L \eta^3 dx + C_{ma} \int_L \eta^4 dx + D_{ma} \int_L \eta^5 dx \right] \quad (10)$$

Similarly the total energy of vibration of the bridge is:

$$\int_L U = \frac{m_p \omega^2}{2} \int_L \eta^2 dx \quad (11)$$

The overall rate of energy change per cycle due to atmospheric damping for the bridge can now be written:

$$\psi_a = \frac{\int_L \Delta U}{\int_L U} = 2 \left[A_{ma} + B_{ma} \frac{\int_L \eta^3 dx}{\int_L \eta^2 dx} + C_{ma} \frac{\int_L \eta^4 dx}{\int_L \eta^2 dx} + D_{ma} \frac{\int_L \eta^5 dx}{\int_L \eta^2 dx} \right] \quad (12)$$

For any mode of oscillation of the bridge the amplitude, η , at any point can be expressed as a function of x ; measured along the longitudinal axis from a convenient point, and of η_0 , the amplitude at any convenient point such as the center of the main span for symmetric modes and the quarter-point of the main span for the first asymmetric mode. Numerical values for the integral ratios for certain wave forms are given in Table 1.

From equation (12) the overall logarithmic decrement of the prototype due to atmospheric damping, δ_{pa} , can be written:

$$\delta_{pa} = \frac{\psi_a}{2} = A_{pa} + B_{pa} \eta_0 + C_{pa} \eta_0^2 + D_{pa} \eta_0^3 \dots \quad (13)$$

in which $A_{pa} = A_{ma}$; $B_{pa} \eta_0 = B_{ma} \frac{\int_L \eta^3 dx}{\int_L \eta^2 dx}$, etc.

If the logarithmic decrement of the bridge, δ_p has been measured in the field or is assumed, it also can be expressed as a power series in η_0 . The structural damping of the bridge, δ_{ps} , can be determined by subtracting δ_{pa} from the total thus:

$$\delta_{ps} = \delta_p - \delta_{pa} \quad (14)$$

If a wind of a certain velocity causes oscillation of the section model the oscillograph record can be analyzed to determine the varying negative values of δ_m for amplitudes below the steady state and its positive values for somewhat higher amplitudes. The structural damping, δ_{ms} , of the section model mounting as determined with the brass rods is subtracted from δ_m to obtain δ_{mav} , the aerodynamic damping in the windstream. This will be expressed:

$$\delta_{mav} = A_{ma} + B_{ma} \eta + C_{ma} \eta^2 + D_{ma} \eta^3 \dots \quad (15)$$

in which numerical values of the coefficients will differ from those in equation (7). Some of them will be negative. Following the process used above for still air damping, an expression similar to equation (13) but with some negative coefficients, will be obtained for δ_{pav} , the overall aerodynamic decrement of the bridge in the prototype wind. The overall decrement, δ_{pv} , of the bridge in the prototype wind will be:

$$\delta_{pv} = \delta_{ps} + \delta_{pav} \quad (16)$$

The prototype amplitude at which $\delta_{pv} = 0$ will be the predicted steady state amplitude, η_0 .

Verification of Theory. Illustrative Example

In order to test this method, predictions based on section model data were compared with the behavior of the full model. Space permits the presentation of only enough of the data to illustrate the procedure and compare the results.

The data used in this illustration are from tests on the model of the new Tacoma Narrows Bridge as modified by covering the roadway slots, removing all of the truss except the top chord, and adding girders 12 ft. deep (prototype). The resulting section had the relative proportions of the original Tacoma Narrows Bridge but was 50% wider and deeper and the suspended structure had several times the vertical stiffness of the original section. Figure 10 shows the cross section of this model.

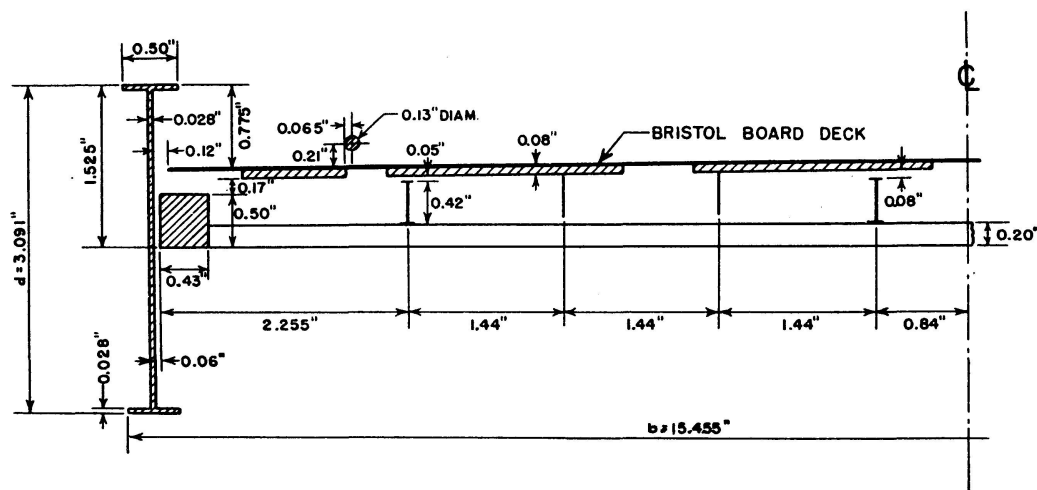


Fig. 10. Model of Girder-Stiffened Bridge

Predictions were made for two vertical modes, the fundamental ($0 - NV$) and the two-node ($2 - NV$). These had natural frequencies of 52.8 cpm and 82.8 cpm respectively. The section model was tested on sets of springs (four to the set) giving natural frequencies of 63.2 cpm and 83.9 cpm, which were used for predictions of the $0 - NV$ and $2 - NV$ modes respectively. Actually tests made at one frequency would have sufficed for both modes because of the consistent relation between model behavior and the V/Nb ratio. Typical calculations for the $0 - NV$ mode are given below.

The logarithmic decrement of the section model in still air, plotted as illustrated in figure 8 is expressed by the equation:

$$\delta_{ms} + \delta_{ma} = 0.01 + 0.026 \eta \quad (17)^8$$

From tests with the brass rods on the same springs the structural damping is:

$$\delta_{ms} + 0.0016 + 0.0005 \eta \quad (18)$$

Subtracting, the atmospheric damping is:

$$\delta_{ma} = 0.0084 + 0.0255 \eta \quad (19)$$

The overall atmospheric damping of the full model (and of the prototype) is obtained by multiplying each term of equation (19) by the proper integral ratio as indicated by equation (12) and the numerical values in Table I for wave form (b) thus:

$$\delta_{fa} = 0.0084 + 0.0255 \times 0.7702 \eta_0 = 0.0084 + 0.0196 \eta_0 \quad (20)$$

(The subscript, f , is used to designate the full model.)

The overall damping of the full model, when oscillated in the fundamental mode in still air was found to correspond to the equation:

$$\delta_{fs} + \delta_{fa} = 0.027 + 0.1436 \eta_0 - 0.0839 \eta_0^2 \quad (21)$$

⁸) This curve not reproduced.

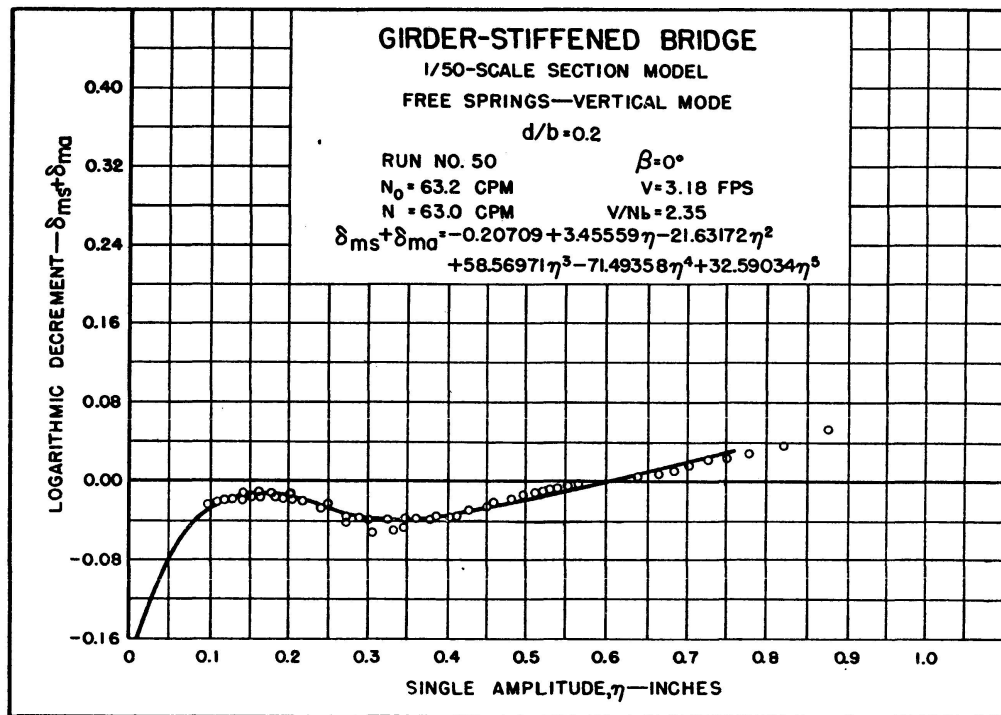


Fig. 11. Logarithmic Decrement for Section Model of Girder-Stiffened Bridge in Wind

Subtracting equation (20) from equation (21) the structural damping of the full model in the $0 - NV$ mode is:

$$\delta_{fs} = 0.0186 + 0.1240 \eta_0 - 0.0839 \eta_0^2 \quad (22)$$

Oscillograph records of the motion of the section model were made at various velocities in a horizontal wind and the logarithmic decrement was computed continuously along these records both above and below the steady state amplitude. Figure 11 shows the plotted points and the equation of the curve for $\delta_{ms} + \delta_{mav}$ as a function of η . Subtracting the structural damping, equation (18), from this gives the net aerodynamic damping:

$$\delta_{mav} = -0.2088 + 3.4551 \eta - 21.6317 \eta^2 + 58.5697 \eta^3 - 71.4936 \eta^4 + 32.5903 \eta^5 \quad (23)$$

This is adjusted to the full model by multiplying the terms by the integral ratios indicated in equation (12) having the numerical values shown in Table 1 for wave form (b) thus:

$$\delta_{fav} = -0.2088 + 2.6611 \eta_0 - 13.5739 \eta_0^2 + 31.0771 \eta_0^3 - 32.9585 \eta_0^4 + 13.3295 \eta_0^5 \quad (24)$$

Finally the overall decrement for the predicted motion of the full model is obtained by adding equations (22) and (24), thus:

$$\delta_{fs} + \delta_{fav} = -0.1902 + 2.7851 \eta_0 - 13.6578 \eta_0^2 + 31.0771 \eta_0^3 - 32.9585 \eta_0^4 + 13.3295 \eta_0^5 \quad (25)$$

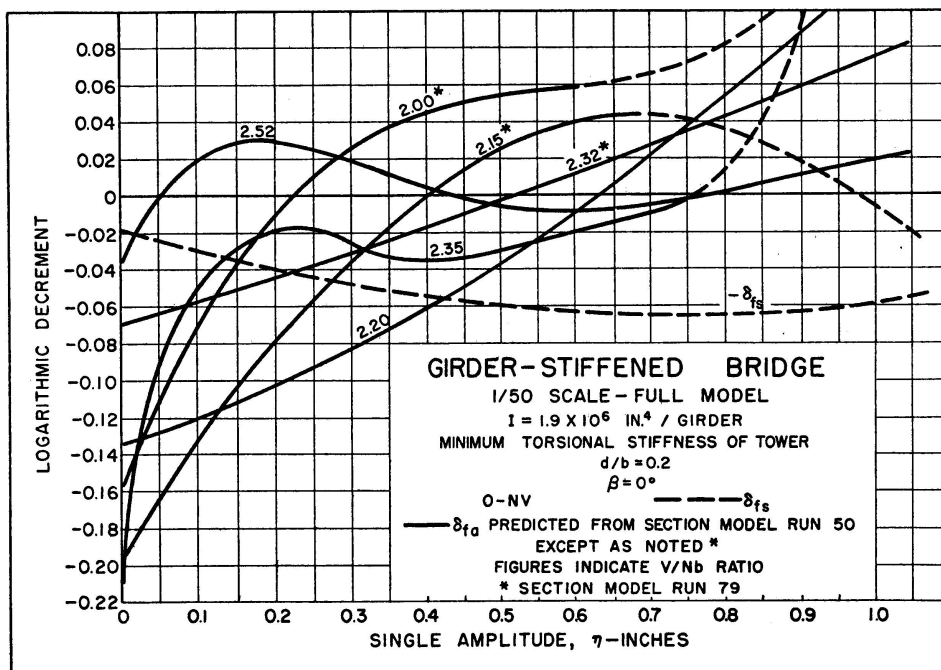


Fig. 12. Predicted Logarithmic Decrements for Full Model of Girder-Stiffened Bridge in Fundamental Vertical Mode

The predicted steady state amplitude of the full model as measured at the center of the main span is the value of η_0 which makes $\delta_{fs} + \delta_{fav} = 0$.

Equation (24) for a wind-velocity of 3.18 fps and a V/Nb ratio of 2.35 is plotted in figure 12 along with curves similarly produced for other velocities and V/Nb ratios. The negative value of equation (22), identified as $-\delta_{fs}$ is plotted as a dashed line. Thus the intersections of this curve with the various full line curves occur at the predicted steady state amplitudes for the V/Nb ratios indicated.

Figure 13 shows similar curves for the two-node vertical mode.

Although the section model was tested on two sets of springs to represent approximately the frequencies of the two modes the results are very nearly the same when plotted against V/Nb ratio instead of velocity. Therefore predictions were made for both modes from both series of section model tests as shown in figures 12 and 13.

Finally, figure 14 shows the double amplitude plotted against the V/Nb ratio for the full model in the two modes for which these predictions were made. The open symbols show predicted points taken from the intersections in figures 12 and 13 (with amplitude doubled) and the solid symbols of the corresponding shape show the amplitudes actually measured on the full model at various wind velocities.

Predictions for the truss-stiffened model with slotted deck did not agree with the observed values as closely as indicated in figure 14 for the girder-

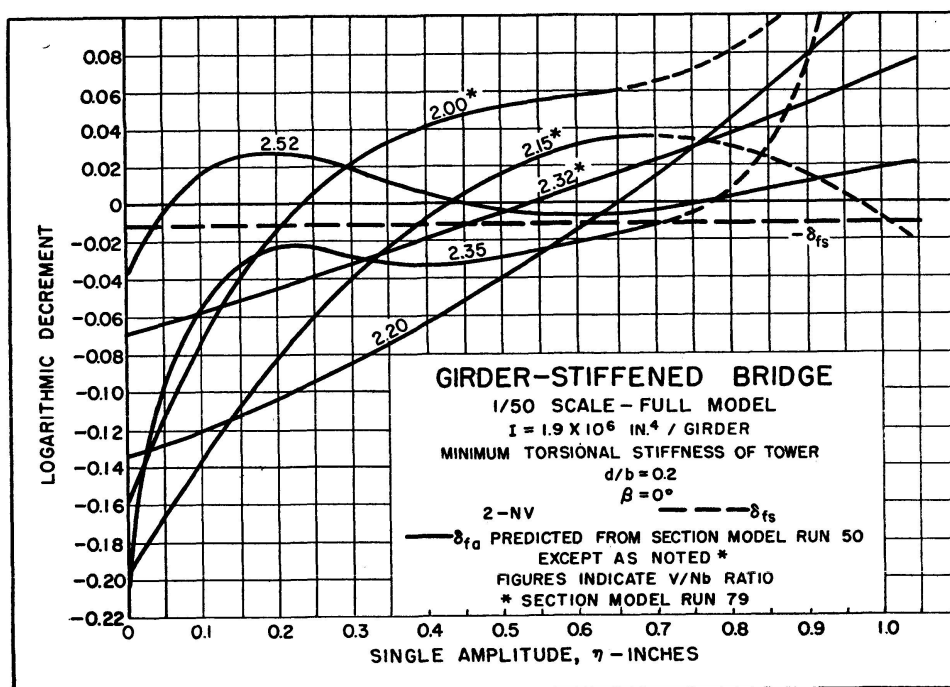


Fig. 13. Predicted Logarithmic Decrements for Full Model of Girder-Stiffened Bridge in Two-Node Vertical Mode

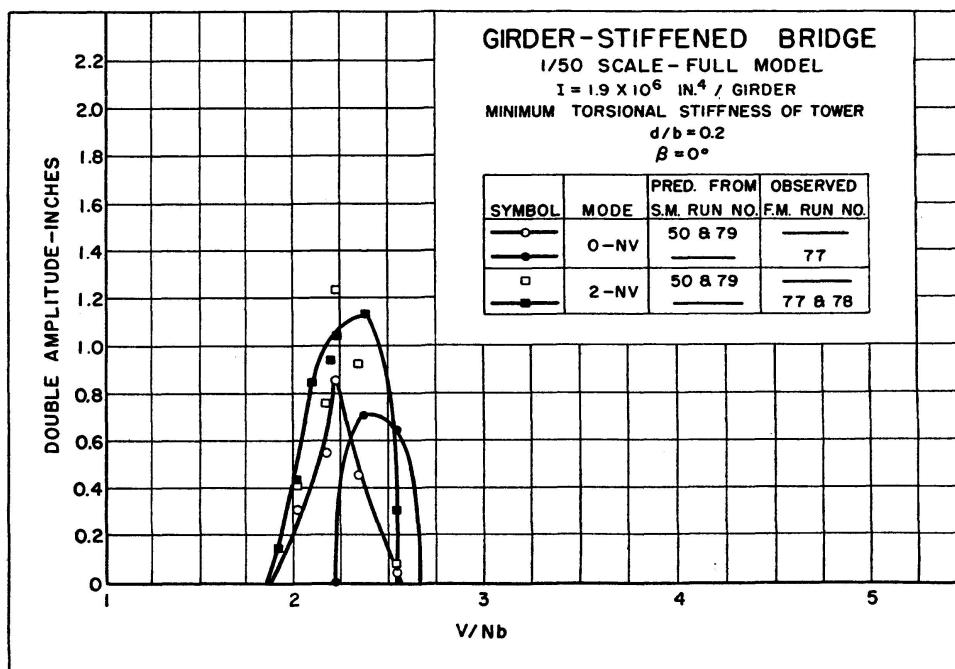


Fig. 14. Predicted and Observed Amplitude Response Curves for Full Model of Girder-Stiffened Bridge in Fundamental and Two-Node Vertical Modes

stiffened model. This is attributed principally to the sensitivity of the truss-stiffened section to angle of attack in winds angled upward about 6° and 8° (the angles used in the tests). As indicated earlier, there was some unavoidable variation in the actual angle along the full model. The agreement was considered close enough to recommend the procedure as a means for ascertaining the probable behavior of a suspension bridge in a known wind. The non-uniformity of natural winds in space and their fluctuation in time reduce their effectiveness in varying degree at different bridge sites so that great refinement in the determination of the response of the bridge in an ideal wind is not essential.

Acknowledgements

The research at the University of Washington and California Institute of Technology on models of the Tacoma Narrows Bridge was sponsored by the Washington Toll Bridge Authority and the United States Bureau of Public Roads, the latter cooperating in the project upon the recommendation of the Advisory Board on the Investigation of Suspension Bridges because of the common interest in the problem. Subsequent extension of the program to the aerodynamic problems of suspension bridges in general was sponsored by the University of Washington and the Bureau of Public Roads. The analytical studies by Dr. FRIEDRICH BLEICH, of which the flutter analysis was only a part⁹⁾, were sponsored by the American Institute of Steel Construction and the Bureau of Public Roads.

Summary

The results of wind tunnel tests on three dimensional models of suspension bridges show sufficient correlation with the behavior of the actual bridges under similar conditions to indicate that the scale effect is small. Static wind tunnel tests on models show that the effect of Reynold's Number on drag, lift and moment is negligible. When the logarithmic decrement for atmospheric damping in model tests in still air is plotted against amplitude of oscillation the resulting curves reveal the action of forces whose strength varies as the square of the velocity with only a small component of viscous damping, indicating that the phenomenon follows Froude's Law. These facts make it possible to use aerodynamic section model tests to predict the behavior of the bridge in the wind.

When a section model, properly scaled as to form, mass and mass distribution, is supported on springs designed to reproduce to scale the vertical,

⁹⁾ "Mathematical Theory of Vibration in Suspension Bridges" by FRIEDRICH BLEICH, C. B. McCULLOUGH, RICHARD ROSECRANS, and GEORGE S. VINCENT. United States Bureau of Public Roads, Government Printing Office.

torsional and coupled movements of the prototype and is exposed in a wind stream, the flow will be similar and the wind forces will be proportional to those associated with the prototype under corresponding conditions. The continuous record of the motion of the model will reveal the integrated work performed on it by the wind forces and will indicate the rate per cycle at which the wind transfers energy to the oscillating system. This rate, which varies with the amplitude, will be the same on the prototype as on the model, the latter representing the conditions over a unit length of the prototype oscillating at a discrete amplitude. The energy transfer per cycle on the prototype can be calculated by integration over the length of the structure using the previously computed frequency and wave form of the mode under investigation. The steady state amplitude in the given wind stream will be that at which the total energy input per cycle just equals that absorbed by the structural damping. The latter, for the prototype, must be known or assumed.

The structural damping of the model mechanism is obtained from tests with equivalent streamlined weights substituted for the section model. When this is subtracted from the damping of the model assembly in still air or a wind-stream the atmospheric damping for that condition is obtained. The tests are extended to sufficient amplitude to include the ranges of positive and negative atmospheric damping. The integration for the prototype is facilitated by expressing the logarithmic decrement as a power series in the amplitude. The curves vary much in form for different velocities.

Zusammenfassung

Die Resultate von Windkanalversuchen mit dreidimensionalen Modellen von Hängebrücken zeigen genügende Übereinstimmung mit dem Verhalten bestehender Brücken, so daß der Einfluß des Maßstabes als klein angenommen werden kann. Aus statischen Windkanalversuchen ergibt sich, daß der Einfluß der Reynold'schen Zahl auf Rücktrieb, Auftrieb und Moment vernachlässigbar ist. Trägt man das logarithmische Dekrement der atmosphärischen Dämpfung des Modellversuchs in unbewegter Luft über der Amplitude der Schwingung auf, so kann aus den entstehenden Kurven abgelesen werden, daß die Größe der wirkenden Kräfte mit dem Quadrate der Geschwindigkeit zunimmt. Die Komponente der viskosen Dämpfung ist nur klein; für den Vorgang ist demnach das Froude'sche Gesetz gültig. Diese Tatsachen ermöglichen es, auf Grund von aerodynamischen Versuchen mit Querschnittsmodellen das Verhalten der Brücke im Wind vorauszusagen.

Wird ein Querschnittsmodell in richtigem Maßstab für Abmessung, Masse und Massenverteilung derart auf Federn gelagert, daß diese die vertikalen,

drehenden und gekoppelten Bewegungen des Prototyps maßstabgetreu nachbilden, so wird im Windkanal die Strömung ähnlich verlaufen und die Windkräfte werden proportional denjenigen sein, wie sie beim Prototyp unter entsprechenden Bedingungen auftreten. Die fortlaufende Aufzeichnung der Bewegungen des Modells ergibt die Integration der von den Windkräften geleisteten Arbeit und gibt an, wieviel Energie der Wind pro Schwingung auf das schwingende System überträgt. Diese Energiemenge, die sich mit der Amplitude ändert, wird dieselbe sein für Prototyp und Modell, da ja das letztere die Bedingungen über die Längeneinheit des mit einer bestimmten Amplitude schwingenden Prototyps darstellt. Der Energieübergang auf den Prototyp pro Periode kann durch Integration über die Länge des Bauwerks berechnet werden unter Verwendung der vorher berechneten Frequenz und Wellenform des zu erforschenden Systems. Die gleichbleibende Amplitude im gegebenen Windstrom wird diejenige sein, bei der die gesamte pro Schwingung zugeführte Energie gerade gleich groß ist, wie die von der mechanischen Dämpfung aufgenommene. Die letztere muß für den Prototyp bekannt sein oder angenommen werden.

Die mechanische Dämpfung des Modellmechanismus wird aus Versuchen mit gleichwertigen stromlinienförmigen Gewichten an Stelle des Querschnittsmodells erhalten. Wird diese subtrahiert von der Dämpfung des zusammengesetzten Modells in stiller Luft oder in einem Windstrom, so erhält man die atmosphärische Dämpfung für diese Bedingungen. Die Versuche werden bis zu genügend großer Amplitude ausgedehnt, um die Bereiche positiver und negativer atmosphärischer Dämpfung zu erfassen. Die Integration für den Prototyp wird erleichtert, wenn man das logarithmische Dekrement als eine Potenzreihe in Funktion der Amplitude ausdrückt. Die Kurven weichen für verschiedene Geschwindigkeiten in ihrer Form stark voneinander ab.

Résumé

Les résultats des essais en soufflerie sur modèles à trois dimensions de ponts suspendus présentent une corrélation suffisamment bonne avec le comportement des ponts réels, dans des conditions semblables, pour que l'on puisse en conclure à une faible influence de la réduction du modèle. Les essais statiques sur modèles, en soufflerie, montrent que l'influence du nombre de Reynold sur la traînée, la portance et le moment est négligeable. Lorsque l'on porte le décrement logarithmique de l'amortissement atmosphérique qui se manifeste au cours d'essais sur modèles, en air calme, en fonction de l'amplitude d'oscillation, les courbes obtenues mettent en évidence l'action de forces qui varient comme le carré de la vitesse, en ne comportant qu'une faible composante d'amortissement visqueux, indiquant que le phénomène suit la loi de Froude.

Ces faits rendent possible l'emploi des essais aérodynamiques sur modèles de sections, pour prévoir le comportement des ponts sous l'effet du vent.

Lorsqu'un modèle de section, correctement proportionné en ce qui concerne la forme, la masse et la distribution des masses est monté sur des ressorts établis de manière à reproduire à l'échelle les mouvements verticaux, torsionnels et combinés du prototype et que ce modèle est exposé à un courant d'air, l'écoulement et les efforts dûs au vent sont similaires à l'écoulement et aux efforts qui se manifestent sur le prototype dans des conditions correspondantes. L'enregistrement continu du mouvement du modèle révèle le travail intégré qui s'accomplit sur lui sous l'action du vent et indique le taux par cycle suivant lequel le vent transfère son énergie au système oscillant. Ce taux, qui varie avec l'amplitude, est le même sur le prototype que sur le modèle et représente les conditions qui se manifestent sur l'unité de longueur du prototype, oscillant sous une amplitude discrète. Le transfert d'énergie par cycle sur le prototype lui-même peut être calculé par intégration sur la longueur de l'ouvrage en utilisant la fréquence et la forme d'onde antérieurement calculées d'après le mode en cours d'examen. L'amplitude en régime stationnaire dans le vent donné est celle qui, sous l'apport total d'énergie par cycle, est juste égale à celle qui se trouve absorbée par l'amortissement de l'ouvrage. Cette dernière doit être connue ou supposée pour le prototype lui-même.

L'amortissement structural du mécanisme modèle est obtenu à partir d'essais effectués à l'aide de poids carénés équivalents substitués au modèle de la section. En déduisant cet amortissement de celui de l'assemblage du modèle en air calme ou dans un courant d'air, on obtient l'amortissement atmosphérique pour la condition considérée. Les essais sont étendus à une amplitude suffisante pour englober les gammes d'amortissements atmosphériques positifs et négatifs. L'intégration relative au prototype est facilitée lorsque l'on exprime le décrétement logarithmique sous la forme d'une série de puissance en amplitude. La forme des courbes varie beaucoup pour les différentes vitesses.